Automatica 101 (2019) 96–102

Contents lists available at ScienceDirect

Automatica

journal homepage: www.elsevier.com/locate/automatica

Brief paper

Connections between control allocation and linear quadratic control for weakly redundant systems☆

Molong Duan, Chinedum E. Okwudire *

Mechanical Engineering Department, University of Michigan, 2350 Hayward, Ann Arbor, MI, 48109, US

ARTICLE INFO

Article history:
Received 26 December 2017
Received in revised form 15 August 2018
Accepted 20 November 2018
Available online xxxx

Keywords:
Linear quadratic control
Over-actuated system
Weak input redundancy

ABSTRACT

In this paper, connections between the control allocation and linear quadratic (LQ) control frameworks for optimally distributing control inputs in weakly input redundant systems are explored. It is also shown that, for a representative class of exogenous disturbance and reference signals, the LQ control technique is identical to the so-called optimal control subspace-based (OCS) control allocation technique. However, for this equivalence to hold, the OCS control allocation technique requires evaluation of a (generally) non-causal relationship between control inputs, while the LQ control technique requires perfect knowledge of the system, disturbance and reference states. In practice, neither of these conditions is achievable; therefore, approximations are needed. In this regard, the OCS control allocation technique is superior because it is explicit about the relationship that must be accurately approximated to attain optimality; this enables good approximations of the optimal relationship to be realized. Conversely, the LQ control technique implicitly approximates the optimal relationship via estimation of states, disturbances and/or reference signals. In a comparison with a classical example based on the Kalman filter, the OCS control allocation is shown to be superior in preserving the optimal alignment of redundant control inputs, thus introducing enhanced performance with reduced cost.

1. Introduction

In over-actuated systems, more actuators are used compared to the outputs to be controlled (Schneiders, Molengraft, & Steinbuch, 2004). Over-actuation (or actuation redundancy) is beneficial in many practical applications, due to its capability to incorporate additional control objectives, or to reduce tradeoffs in optimal solutions. For example, redundant actuators are employed in aircrafts to enhance the fault tolerance (Servidia & Pena, 2005). In servo systems, the use of redundant actuators enhances motion accuracy (Brinkerhoff & Devasia, 2000), motion range (Zheng, Su, & Fu, 2010), energy efficiency (Halevi, Carpanzano, & Montalbano, 2014), and the ability to suppress structural resonances (Ronde, Schneiders, Kikken, van de Molengraft, & Steinbuch, 2014).

Despite its advantages, over-actuation brings additional challenges, chief of which is optimal allocation of control inputs among the redundant actuators (Johansen & Fossen, 2013). The criterion for determining optimal allocation of control inputs varies from problem to problem. However, one common metric for optimally allocating control inputs is the weighted two norm of the control inputs (Bodson, 2002; Chen & Wang, 2014; Härkegård, 2004; Härkegård & Glad, 2005; Johansen & Fossen, 2013; Petersen & Bodson, 2006; Tagesson, Sundstrom, Laine, & Dela, 2009; Zaccarian, 2009; Zhou, Canova, & Serrani, 2016). This metric is often combined with other control performance requirements, e.g., tracking or regulation performance. Perhaps the most well-known example is linear quadratic (LQ) control (Anderson & Moore, 1971), where control performance and control energy formulate conflicting objectives that must be traded off. The introduction of redundant control inputs has been shown to enhance controllability in the LQ control framework (Duan, Huang, Yao, & Jiang, 2012). However, in general, the LQ control framework does not distinguish between over-actuated and non-over-actuated systems, and thus does not explicitly capture the characteristics of over-actuated systems. Accordingly, the conflicting objectives are coupled, which, in general, complicates the selection (or tuning) of weights.

A more tailored approach for optimally allocating control inputs in over-actuated systems is referred to in the literature as control allocation. Taking advantage of the redundancy, control allocation decouples the control design process into two stages. First, a high level non-redundant 'virtual controller' enforces the desired control performance without worrying about how the required control

☆ This work is funded by the National Science Foundation's CAREER Award #1350202: Dynamically Adaptive Feed Drives for Smart and Sustainable Manufacturing. The material in this paper was not presented at any conference. This paper was recommended for publication in revised form by Associate Editor Akira Kojima under the direction of Editor Ian R. Petersen.

* Corresponding author.
E-mail addresses: molong@umich.edu (M. Duan), okwudire@umich.edu (C.E. Okwudire).

https://doi.org/10.1016/j.automatica.2018.11.049
0005-1098/

efforts are allocated. Subsequently, a low level control allocator distributes the control efforts based on the virtual control, while addressing the additional control objectives (Chen & Wang, 2014; Härkegård, 2004; Härkegård & Glad, 2005; Johansen & Fossen, 2013).

Prior research on control allocation has mainly focused on strongly input redundant systems, where there exists a set of control inputs that do not affect a system's internal states (Bodson, 2002; Härkegård, 2004; Härkegård & Glad, 2005; Petersen & Bodson, 2006). However, strong input redundancy is restrictive in practice, since it often requires exact collocation of actuators or severe truncation of higher order dynamics (Härkegård, 2004). Weak input redundancy is a more practically tenable problem, where there exists a set of control inputs that do not affect the system's outputs, though they may alter some of its internal states (Galeani & Pettinari, 2014; Galeani, Serrani, Varano, & Zaccarian, 2015; Zaccarian, 2009; Zhou et al., 2016). Control allocation for weakly input redundant systems is more general and challenging, since the relationship among the redundant actuators is no longer static. Available methods include model predictive control (Zhou et al., 2016), gain matrix scheduling (Galeani et al., 2015), gradient-based hybrid system for multi-sinusoidal exogenous inputs (Galeani & Pettinari, 2014), and static redundancy model approximation (Zaccarian, 2009). Recently, the authors introduced a new class of methods that perform control allocation based on the existence of an optimal control subspace in weakly redundant systems (Duan & Okwudire, 2016a,b, 2017, 2018). The optimal control subspace specifies the relationship of the redundant inputs to stay optimal regardless of reference and disturbance. Based on this relationship, optimal control subspace-based (OCS) control allocation is shown to facilitate broadband control allocation for weakly redundant systems, without need for computationally expensive real-time optimization.

Given the availability of the LQ and control allocation frameworks for optimal distribution of control efforts in over-actuated systems, a question that arises is how these two frameworks may be related. The connection between the LQ approach and control allocation is discussed in (Härkegård & Glad, 2005). It is shown that the two approaches yield identical solutions for strongly input redundant systems. However, the relationship between the two approaches for weakly input redundant systems was not explored. The original contributions of this work are, therefore, in: (i) deriving the optimal solution structure for the OCS control allocation for weakly input redundant systems, and showing its equivalence to the LQ approach; (ii) highlighting fundamental challenges in implementing the optimal solution for both LQ and OCS control allocation techniques, and the need for approximations; and (iii) showing that, compared to the LQ approach, OCS control allocation is more explicit about the criterion for optimal allocation, hence it lends itself better to near-optimal approximations. The key conclusion of this work is that the control allocation framework (specifically the OCS technique) is a more general and practical means of achieving (near) optimal control allocation for weakly redundant systems compared to the LQ framework.

The rest of this paper is organized as follows: Background knowledge on control allocation and LQ control for weakly redundant systems is provided in Section 2. The optimal solution structure and the equivalence proof for OCS control allocation and LQ control are discussed in Section 3. This is followed by a discussion of approximations to the optimal solution and simulation examples in Section 4, as well as conclusions in Section 5.

2. Background

Assume a strictly proper linear time invariant multi-input, multi-output system (as shown in Fig. 1) given by

$$\mathbf{y} = \mathbf{G}(s)\,\mathbf{u} + \mathbf{G}_{\mathrm{d}}(s)\,\mathbf{d}, \tag{1}$$

where $\mathbf{y} \in \mathbb{R}^{n_{\mathrm{y}}}$ is the output of the system, while $\mathbf{u} \in \mathbb{R}^{n_{\mathrm{u}}}$, $\mathbf{d} \in \mathbb{R}^{n_{\mathrm{d}}}$ are the control input and disturbance, respectively. Assume that one minimal state-space realization of the system is given by

$$\begin{aligned} \dot{\mathbf{x}} &= \mathbf{A}\mathbf{x} + \mathbf{B}_1\mathbf{u} + \mathbf{B}_2\mathbf{d}; \\ \mathbf{y} &= \mathbf{C}\mathbf{x}. \end{aligned} \tag{2}$$

where $\mathbf{x} \in \mathbb{R}^{n_{\mathrm{x}}}$ is the state vector of the system.

Definition 1. The system given by (1) and (2) is:
(a) strongly input redundant if

$$\mathrm{Ker}\,(\mathbf{B}_1) \neq \{\mathbf{0}\}; \tag{3}$$

(b) weakly input redundant if

$$\mathrm{Ker}\,(\mathbf{G}(s)) \neq \{\mathbf{0}\}, \text{ for all } s. \tag{4}$$

Remark 1. Definition 1 arises from Zaccarian (2009) but is slightly altered in two aspects to fit with the discussion in this paper. Firstly, the system is assumed to be strictly proper such that there is no direct feedthrough term $\mathbf{D}$ in the state-space model. This assumption simplifies the expression, and is consistent with the later-discussed LQ tracking controller. Secondly, the original definition of the weakly input redundant system (Zaccarian, 2009) focused on only static control allocation (i.e., for $s \to 0$). Following (Duan & Okwudire, 2017), this original definition is extended to all frequencies (broadband) as in (4).

Remark 2. The concept of weak input redundancy is more general and practical since it does not require cancellable redundant inputs without affecting the internal states. This generality is also shown from the relationship between state-space and transfer function representations of a system, i.e.,

$$\mathbf{G}(s) = \mathbf{C}\,(s\mathbf{I}-\mathbf{A})^{-1}\,\mathbf{B}_1, \tag{5}$$

strongly input redundant systems formulate a subset of weakly input redundant systems, i.e., (3) $\Rightarrow$ (4). From this point of view, weak input redundancy can also be defined by a larger number of inputs compared to outputs, i.e., $n_{\mathrm{u}} > n_{\mathrm{y}}$. Here we define a positive integer

$$n_{\mathrm{r}} = n_{\mathrm{u}} - n_{\mathrm{y}} \tag{6}$$

to indicate the system's redundancy degree.

2.1. OCS control allocation

The control allocation is a concept to decompose the control into two stages as in Fig. 1: considering both desired and actual output $\mathbf{y}_{\mathrm{d}}$ and $\mathbf{y}$, a non-redundant virtual controller generates virtual control $\boldsymbol{\tau}$ based on requirements on control performances; this virtual control is then distributed into different control channels optimally through control allocator $\mathbf{P}_0$. The core concept of OCS control allocation applies to the design of the control allocator $\mathbf{P}_0$ such that they are optimally distributed without altering $\mathbf{y}$ (as determined via the virtual control $\boldsymbol{\tau}$.

Given that there are more control inputs than outputs in weakly input redundant systems, there exists a subset of n_{y} principal control inputs, which formulate a non-redundant input set. Correspondingly, the over-actuated system is divided as

$$\mathbf{G}(s) = \begin{bmatrix} \mathbf{G}_{\mathrm{p}}(s) & \mathbf{G}_{\mathrm{r}}(s) \end{bmatrix}; \ \mathbf{u} = \begin{bmatrix} \mathbf{u}_{\mathrm{p}}^{\mathrm{T}} & \mathbf{u}_{\mathrm{r}}^{\mathrm{T}} \end{bmatrix}^{\mathrm{T}}, \tag{7}$$

where $\mathbf{G}_{\mathrm{p}}$ is a nonsingular square transfer function matrix from the first n_{y} principal control inputs $\mathbf{u}_{\mathrm{p}}$ to the outputs, and $\mathbf{G}_{\mathrm{r}}$ $(n_{\mathrm{y}} \times n_{\mathrm{r}})$ is a transfer function matrix from the remaining n_{r} redundant control inputs $\mathbf{u}_{\mathrm{r}}$ to the outputs. It is shown in Duan and Okwudire (2017)

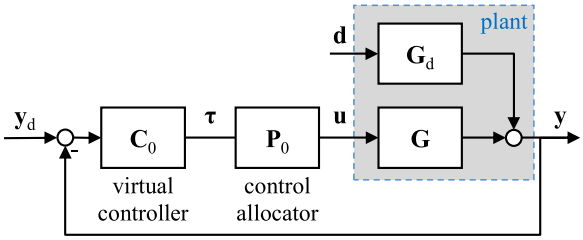

Fig. 1. Block diagram of control allocation in tracking control with exogenous disturbance.

that the optimal control $\hat{\mathbf{u}}$ of such weakly input redundant system, with quadratic control energy cost

$$J_u = \frac{1}{2}\int_0^{+\infty} \begin{bmatrix}\mathbf{u}_p\\ \mathbf{u}_r\end{bmatrix}^T \underbrace{\begin{bmatrix}\mathbf{R}_p & \mathbf{R}_{pr}\\ \mathbf{R}_{pr}^T & \mathbf{R}_r\end{bmatrix}}_{\mathbf{R}} \begin{bmatrix}\mathbf{u}_p\\ \mathbf{u}_r\end{bmatrix} dt, \tag{8}$$

satisfies following relationship

$$\begin{aligned}&\left[\left(\mathbf{G}_p^{-1}\mathbf{G}_r\right)^* \mathbf{R}_p - \mathbf{R}_{pr}^T\right]\hat{\mathbf{u}}_p = \left[\mathbf{R}_r - \left(\mathbf{G}_p^{-1}\mathbf{G}_r\right)^* \mathbf{R}_{pr}\right]\hat{\mathbf{u}}_r\\ &\quad\Leftrightarrow \left[\left(\mathbf{G}_p^{-1}\mathbf{G}_r\right)^* \quad -\mathbf{I}\right]\mathbf{R}\hat{\mathbf{u}} = \mathbf{0},\end{aligned} \tag{9}$$

where * represents the adjoint operation (Beard, 2002) and $\hat{}$ indicates optimality. This relationship formulates the optimal control subspace of weakly input redundant systems.

2.2. LQ controller (with reference tracking and disturbance rejection)

Besides control allocation, another natural thought in handling over-actuated system is to formulate the problem under the LQ control framework.

Problem 1. Assume that $\mathbf{y}_d$ represents the desired output of the system defined in (1) and (2), find optimal $\mathbf{u}$ such that the quadratic objective on tracking performance and control energy, given by

$$J_{uy} = \frac{1}{2}\int_0^{+\infty} \left((\mathbf{y}-\mathbf{y}_d)^T \mathbf{Q}_y (\mathbf{y}-\mathbf{y}_d) + \mathbf{u}^T\mathbf{R}\mathbf{u}\right) dt, \tag{10}$$

is minimized.

Remark 3. The formulation of Problem 1 suits with weak input redundancy since it does not involve the internal states in the objective. However, the results apply to general LQ formulation with weights on state by defining

$$\mathbf{Q} \triangleq \mathbf{C}^T\mathbf{Q}_y\mathbf{C}, \tag{11}$$

such that $\mathbf{x}^T\mathbf{Q}\mathbf{x} = \mathbf{y}^T\mathbf{Q}_y\mathbf{y}$.

Lemma 1 (*Linear Quadratic Tracker*)**.** *Assume the disturbance* $\mathbf{d}$ *and desired output* $\mathbf{y}_d$ *are generated from exo-systems*

$$\dot{\mathbf{d}} = \mathbf{E}\mathbf{d};\ \ \dot{\boldsymbol{\omega}} = \mathbf{F}\boldsymbol{\omega};\ \ \mathbf{y}_d = \mathbf{C}_y\boldsymbol{\omega} \tag{12}$$

where $\mathbf{E}$ *and* $\mathbf{F}$ *are square matrices with no eigenvalue on the right half-plane, and* $\mathbf{C}_y$ *is a reference output matrix. Assume matrix* $\mathbf{A}$ *is Hurwitz, the optimal solution* $\hat{\mathbf{u}}$ *to Problem 1 satisfies following feedback and feedforward structure:*

$$\begin{aligned}&\hat{\mathbf{u}} = -\mathbf{R}^{-1}\mathbf{B}_1^T\mathbf{p};\\ &\mathbf{p} = \mathbf{P}_1\mathbf{x} + \mathbf{P}_2\mathbf{d} + \mathbf{P}_3\boldsymbol{\omega},\end{aligned} \tag{13}$$

where the $\mathbf{P}_1$, $\mathbf{P}_2$, *and* $\mathbf{P}_3$ *satisfy the Riccati equation (14) and Sylvester equations (15)(16) as*

$$\mathbf{A}^T\mathbf{P}_1 + \mathbf{P}_1\mathbf{A} - \mathbf{P}_1\mathbf{B}_1\mathbf{R}^{-1}\mathbf{B}_1^T\mathbf{P}_1 + \mathbf{Q} = \mathbf{0}: \tag{14}$$

$$\mathbf{A}_{cl}^T\mathbf{P}_2 + \mathbf{P}_2\mathbf{E} = -\mathbf{P}_1\mathbf{B}_2; \tag{15}$$

$$\mathbf{A}_{cl}^T\mathbf{P}_3 + \mathbf{P}_3\mathbf{F} = \mathbf{C}^T\mathbf{Q}_y\mathbf{C}_y. \tag{16}$$

Matrix $\mathbf{A}_{cl}$ is part of the closed-loop state-space model, i.e.

$$\mathbf{A}_{cl} \triangleq \mathbf{A} - \mathbf{B}_1\mathbf{R}^{-1}\mathbf{B}_1^T\mathbf{P}_1. \tag{17}$$

The solutions to Sylvester equations (15)(16) are unique if $\mathbf{A}_{cl}$ shares no common eigenvalues with $\mathbf{E}$ and $\mathbf{F}$.

Remark 4. Lemma 1, which applies to infinite length $\mathbf{d}$ and $\mathbf{y}_d$ in continuous system, is a natural extension of the optimal control of finite length $\mathbf{d}$ and $\mathbf{y}_d$, as discussed in Bryson and Ho (1975) and Singh and Pal (2017).

3. Main result

In this section, it is shown that the LQ solution for a weakly redundant system, including general external disturbances and desired output tracking, formulates a two-stage structure as in control allocation. It is also shown that the optimal state feedback in (13) also yields the two-stage control allocation structure.

Theorem 1. *The optimal solution* $\hat{\mathbf{u}}$ *to Problem 1 satisfies the following two-stage control allocation structure:*

$$\hat{\mathbf{u}} = \mathbf{R}^{-1}\mathbf{G}^*\boldsymbol{\tau}; \tag{18}$$

$$\boldsymbol{\tau} = \mathbf{Q}_y(\mathbf{y}_d - \mathbf{y}). \tag{19}$$

Proof. According to Pontryagin's minimum principle (Kirk, 2012), the Hamiltonian of the system is written as

$$\begin{aligned}H = &\frac{1}{2}\left(\left(\mathbf{x}^T\mathbf{C}^T - \mathbf{y}_d^T\right)\mathbf{Q}_y(\mathbf{C}\mathbf{x} - \mathbf{y}_d) + \mathbf{u}^T\mathbf{R}\mathbf{u}\right)\\ &+ \mathbf{p}^T(\mathbf{A}\mathbf{x} + \mathbf{B}_1\mathbf{u} + \mathbf{B}_2\mathbf{d}),\end{aligned} \tag{20}$$

where $\mathbf{p}$ is a vector of co-states. The co-states are crucial to the optimal solution because

$$\frac{\partial H}{\partial \mathbf{u}}(\hat{\mathbf{u}}) = 0 \Rightarrow \mathbf{R}\hat{\mathbf{u}} + \mathbf{B}_1^T\mathbf{p} = \mathbf{0} \Rightarrow \hat{\mathbf{u}} = -\mathbf{R}^{-1}\mathbf{B}_1^T\mathbf{p}. \tag{21}$$

The combination of state and co-state dynamics is written as

$$\begin{aligned}&\frac{d}{dt}\begin{bmatrix}\mathbf{x}\\ \mathbf{p}\end{bmatrix} = \begin{bmatrix}\frac{\partial H}{\partial \mathbf{p}}\\ -\frac{\partial H}{\partial \mathbf{x}}\end{bmatrix} = \mathbf{M}\begin{bmatrix}\mathbf{x}\\ \mathbf{p}\end{bmatrix} + \begin{bmatrix}\mathbf{B}_2\\ \mathbf{0}\end{bmatrix}\mathbf{d} + \begin{bmatrix}0\\ \mathbf{C}^T\mathbf{Q}_y\end{bmatrix}\mathbf{y}_d,\\ &\mathbf{M} \triangleq \begin{bmatrix}\mathbf{A} & -\mathbf{B}_1\mathbf{R}^{-1}\mathbf{B}_1^T\\ -\underbrace{\mathbf{C}^T\mathbf{Q}_y\mathbf{C}}_{\mathbf{Q}} & -\mathbf{A}^T\end{bmatrix}.\end{aligned} \tag{22}$$

Using Laplace transform, both $\mathbf{x}$ and $\mathbf{p}$ can be expressed as outputs relative to $\mathbf{d}$ and $\mathbf{y}_d$. The co-state is expressed as

$$\mathbf{p} = \begin{bmatrix}\mathbf{0} & \mathbf{I}\end{bmatrix}\begin{bmatrix}\mathbf{x}\\ \mathbf{p}\end{bmatrix} = \begin{bmatrix}\mathbf{0} & \mathbf{I}\end{bmatrix}\mathbf{N}\left(\begin{bmatrix}\mathbf{B}_2\\ \mathbf{0}\end{bmatrix}\mathbf{d} + \begin{bmatrix}0\\ \mathbf{C}^T\mathbf{Q}_y\end{bmatrix}\mathbf{y}_d\right), \tag{23}$$

where $\mathbf{N} \triangleq (s\mathbf{I}-\mathbf{M})^{-1}$. In $\mathbf{N}$, only N_{21} and N_{22} contribute to the co-states, i.e.

$$\mathbf{p} = N_{21}\mathbf{B}_2\mathbf{d} + N_{22}\mathbf{C}^T\mathbf{Q}_y\mathbf{y}_d, \tag{24}$$

which can be analytically determined through the block-wise matrix inversion formula (Petersen & Pedersen, 2008) as

$$\begin{aligned}N_{21} = &-\left(s\mathbf{I} + \mathbf{A}^T\right)^{-1}\cdot\\ &\mathbf{Q}\left(s\mathbf{I} - \mathbf{A} - \mathbf{B}_1\mathbf{R}^{-1}\mathbf{B}_1^T\left(s\mathbf{I} + \mathbf{A}^T\right)^{-1}\mathbf{Q}\right)^{-1};\\ N_{22} = &\left(s\mathbf{I} + \mathbf{A}^T - \mathbf{Q}(s\mathbf{I} - \mathbf{A})^{-1}\mathbf{B}_1\mathbf{R}^{-1}\mathbf{B}_1^T\right)^{-1}.\end{aligned} \tag{25}$$

Using the relationship in (5) and the definition of the adjoint of system dynamics (Kothare & Morari, 1996)

$$\mathbf{G}^*(s) = -\mathbf{B}_1^{\mathrm{T}}\left(s\mathbf{I} + \mathbf{A}^{\mathrm{T}}\right)^{-1}\mathbf{C}^{\mathrm{T}}, \tag{26}$$

the optimal control in (21) yields

$$\begin{aligned}\hat{\mathbf{u}} = &-\mathbf{R}^{-1}\mathbf{B}_1^{\mathrm{T}}\left(s\mathbf{I} + \mathbf{A}^{\mathrm{T}} - \mathbf{C}^{\mathrm{T}}\mathbf{Q}_{\mathrm{y}}\mathbf{G}\mathbf{R}^{-1}\mathbf{B}_1^{\mathrm{T}}\right)^{-1}\mathbf{C}^{\mathrm{T}}\mathbf{Q}_{\mathrm{y}}\mathbf{y}_{\mathrm{d}}\\ &-\mathbf{R}^{-1}\mathbf{G}^*\mathbf{Q}_{\mathrm{y}}\mathbf{C}\left(s\mathbf{I} - \mathbf{A} + \mathbf{B}_1\mathbf{R}^{-1}\mathbf{G}^*\mathbf{Q}_{\mathrm{y}}\mathbf{C}\right)^{-1}\mathbf{B}_2\mathbf{d}.\end{aligned} \tag{27}$$

Note that the inversions in (27) can be simplified using the Woodbury matrix identity formula, i.e.

$$\begin{aligned}&\hat{\mathbf{u}} = \mathbf{R}^{-1}\mathbf{G}^*\boldsymbol{\tau};\\ &\boldsymbol{\tau} = -\mathbf{Q}_{\mathrm{y}}\left(\mathbf{I} + \mathbf{G}_\tau\mathbf{Q}_{\mathrm{y}}\right)^{-1}\mathbf{G}_{\mathrm{d}}\mathbf{d} + \left(\mathbf{I} + \mathbf{Q}_{\mathrm{y}}\mathbf{G}_\tau\right)^{-1}\mathbf{Q}_{\mathrm{y}}\mathbf{y}_{\mathrm{d}},\end{aligned} \tag{28}$$

where $\tau \in \mathbb{R}^{n_{\mathrm{y}}}$ is defined as virtual control input and

$$\mathbf{G}_\tau \triangleq \mathbf{G}(s)\mathbf{R}^{-1}\mathbf{G}^*(s). \tag{29}$$

Replacing $\mathbf{G}_{\mathrm{d}}\mathbf{d}$ with $\mathbf{y}$–$\mathbf{G}_\tau\tau$ in (28) and applying Woodbury matrix identity formula, the expression of τ can be simplified as

$$\begin{aligned}&\left(\mathbf{I} - \mathbf{Q}_{\mathrm{y}}\left(\mathbf{I} + \mathbf{G}_\tau\mathbf{Q}_{\mathrm{y}}\right)^{-1}\mathbf{G}_\tau\right)\boldsymbol{\tau} = \left(\mathbf{I} + \mathbf{Q}_{\mathrm{y}}\mathbf{G}_\tau\right)^{-1}\boldsymbol{\tau}\\ &= -\mathbf{Q}_{\mathrm{y}}\left(\mathbf{I} + \mathbf{G}_\tau\mathbf{Q}_{\mathrm{y}}\right)^{-1}\mathbf{y} + \left(\mathbf{I} + \mathbf{Q}_{\mathrm{y}}\mathbf{G}_\tau\right)^{-1}\mathbf{Q}_{\mathrm{y}}\mathbf{y}_{\mathrm{d}}\\ &\Rightarrow \boldsymbol{\tau} = -\left(\mathbf{I} + \mathbf{Q}_{\mathrm{y}}\mathbf{G}_\tau\right)\mathbf{Q}_{\mathrm{y}}\left(\mathbf{I} + \mathbf{G}_\tau\mathbf{Q}_{\mathrm{y}}\right)^{-1}\mathbf{y} + \mathbf{Q}_{\mathrm{y}}\mathbf{y}_{\mathrm{d}}\\ &= \mathbf{Q}_{\mathrm{y}}\left(\mathbf{y}_{\mathrm{d}} - \mathbf{y}\right).\end{aligned} \tag{30}$$

This is identical to the expression shown in (18)(19). ■

Remark 5. Theorem 1 indicates that the optimal solution to Problem 1 yields a natural two-stage structure, where the tracking objective and the energy objective can be decoupled. This also shows that the two-stage structure in control allocation does not sacrifice optimality for weak input redundancy.

Theorem 2. *The feedback/feedforward solution specified in Lemma 1 satisfies the control allocation structure in Theorem 1.*

Proof. The state dynamics of the corresponding system in closed loop is given by

$$\dot{\mathbf{x}} = \mathbf{A}_{\mathrm{cl}}\mathbf{x} + \mathbf{B}_{\mathrm{cl,d}}\mathbf{d} + \mathbf{B}_{\mathrm{cl,y}}\boldsymbol{\omega}, \tag{31}$$

where

$$\begin{aligned}&\mathbf{B}_{\mathrm{cl,d}} = \mathbf{B}_2 - \mathbf{B}_1\mathbf{R}^{-1}\mathbf{B}_1^{\mathrm{T}}\mathbf{P}_2;\\ &\mathbf{B}_{\mathrm{cl,y}} = -\mathbf{B}_1\mathbf{R}^{-1}\mathbf{B}_1^{\mathrm{T}}\mathbf{P}_3.\end{aligned} \tag{32}$$

The state dynamics of this system is expressed as

$$\begin{aligned}\mathbf{x}(t) &= \int_0^t e^{\mathbf{A}_{\mathrm{cl}}(t-\tau)}\left(\mathbf{B}_{\mathrm{cl,d}}\mathbf{d}(\tau) + \mathbf{B}_{\mathrm{cl,y}}\boldsymbol{\omega}(\tau)\right)d\tau\\ &= \left(\mathbf{P}_4e^{\mathbf{E}t} - e^{\mathbf{A}_{\mathrm{cl}}t}\mathbf{P}_4\right)\mathbf{d}_0 + \left(\mathbf{P}_5e^{\mathbf{F}t} - e^{\mathbf{A}_{\mathrm{cl}}t}\mathbf{P}_5\right)\boldsymbol{\omega}_0,\end{aligned} \tag{33}$$

where $\mathbf{d}_0$ and $\boldsymbol{\omega}_0$ are the initial values of $\mathbf{d}$ and $\boldsymbol{\omega}$, respectively; $\mathbf{P}_4$ and $\mathbf{P}_5$ are matrices satisfying following Sylvester equations

$$\mathbf{P}_4\mathbf{E} - \mathbf{A}_{\mathrm{cl}}\mathbf{P}_4 = \mathbf{B}_{\mathrm{cl,d}}; \tag{34}$$

$$\mathbf{P}_5\mathbf{F} - \mathbf{A}_{\mathrm{cl}}\mathbf{P}_5 = \mathbf{B}_{\mathrm{cl,y}}. \tag{35}$$

Accordingly, the optimal control is expressed as

$$\begin{aligned}\mathbf{u} = &-\mathbf{R}^{-1}\mathbf{B}_1^{\mathrm{T}}\{[(\mathbf{P}_1\mathbf{P}_4 + \mathbf{P}_2)e^{\mathbf{E}t} - \mathbf{P}_1e^{\mathbf{A}_{\mathrm{cl}}t}\mathbf{P}_4]\mathbf{d}_0\\ &+ [(\mathbf{P}_1\mathbf{P}_5 + \mathbf{P}_3)e^{\mathbf{F}t} - \mathbf{P}_1e^{\mathbf{A}_{\mathrm{cl}}t}\mathbf{P}_5]\boldsymbol{\omega}_0\}.\end{aligned} \tag{36}$$

From the control allocation structure, the adjoint system can be evaluated through convolution as

$$\begin{aligned}&\mathbf{R}^{-1}\mathbf{G}^*\mathbf{Q}_{\mathrm{y}}\left(\mathbf{y}_{\mathrm{d}} - \mathbf{y}\right)\\ &= \mathbf{R}^{-1}\mathbf{B}_1^{\mathrm{T}}e^{-\mathbf{A}^{\mathrm{T}}t}\int_t^{+\infty}e^{\mathbf{A}^{\mathrm{T}}\sigma}\mathbf{C}^{\mathrm{T}}\mathbf{Q}_{\mathrm{y}}\left(\mathbf{C}_{\mathrm{y}}\boldsymbol{\omega}(\sigma) - \mathbf{C}\mathbf{x}(\sigma)\right)d\sigma\\ &= \mathbf{R}^{-1}\mathbf{B}_1^{\mathrm{T}}e^{-\mathbf{A}^{\mathrm{T}}t}\left\{\int_t^{+\infty}e^{\mathbf{A}^{\mathrm{T}}\sigma}\left(\mathbf{Q}e^{\mathbf{A}_{\mathrm{cl}}\sigma}\mathbf{P}_4 - \mathbf{Q}\mathbf{P}_4e^{\mathbf{E}\sigma}\right)d\sigma\,\mathbf{d}_0\right.\\ &\left.+\int_t^{+\infty}e^{\mathbf{A}^{\mathrm{T}}\sigma}\left(\left(\mathbf{Q}\mathbf{P}_5 - \mathbf{C}^{\mathrm{T}}\mathbf{Q}_{\mathrm{y}}\mathbf{C}_{\mathrm{y}}\right)e^{\mathbf{F}\sigma} - \mathbf{Q}e^{\mathbf{A}_{\mathrm{cl}}\sigma}\mathbf{P}_5\right)d\sigma\,\boldsymbol{\omega}_0\right\}.\end{aligned} \tag{37}$$

This integration can be simplified with two equations

$$\mathbf{A}^{\mathrm{T}}\left(\mathbf{P}_1\mathbf{P}_4 + \mathbf{P}_2\right) + \left(\mathbf{P}_1\mathbf{P}_4 + \mathbf{P}_2\right)\mathbf{E} = -\mathbf{Q}\mathbf{P}_4; \tag{38}$$

$$\mathbf{A}^{\mathrm{T}}\left(\mathbf{P}_1\mathbf{P}_5 + \mathbf{P}_3\right) + \left(\mathbf{P}_1\mathbf{P}_5 + \mathbf{P}_3\right)\mathbf{F} = -\mathbf{Q}\mathbf{P}_5 + \mathbf{C}^{\mathrm{T}}\mathbf{Q}_{\mathrm{y}}\mathbf{C}_{\mathrm{y}}, \tag{39}$$

which can be conveniently shown from the Riccati equation (14) and Sylvester equations (15), (16), (34), and (35). Accordingly,

$$\frac{d}{dt}\left(e^{\mathbf{A}^{\mathrm{T}}t}\left(\mathbf{P}_1\mathbf{P}_4 + \mathbf{P}_2\right)e^{\mathbf{E}t}\right) = -e^{\mathbf{A}^{\mathrm{T}}t}\mathbf{Q}\mathbf{P}_4e^{\mathbf{E}t}; \tag{40}$$

$$\frac{d}{dt}\left(e^{\mathbf{A}^{\mathrm{T}}t}\left(\mathbf{P}_1\mathbf{P}_5 + \mathbf{P}_3\right)e^{\mathbf{F}t}\right) = e^{\mathbf{A}^{\mathrm{T}}t}\left(\mathbf{C}^{\mathrm{T}}\mathbf{Q}_{\mathrm{y}}\mathbf{C}_{\mathrm{y}} - \mathbf{Q}\mathbf{P}_5\right)e^{\mathbf{F}t}. \tag{41}$$

These relationships simplify the integration in (37) and lead to

$$\hat{\mathbf{u}} = \mathbf{R}^{-1}\mathbf{G}^*\mathbf{Q}_{\mathrm{y}}\left(\mathbf{y}_{\mathrm{d}} - \mathbf{y}\right), \tag{42}$$

which is the structure specified in Theorem 1. ■

Remark 6. The expression for $\hat{\mathbf{u}}$ in (18) satisfies the optimal control subspace specified in (9). Accordingly, Theorem 2 indicates that the LQ solution with perfectly known disturbance and reference models satisfies the two-stage structure of OCS control allocation. Note that the OCS control allocation does not require the disturbance to be generated using exo-systems, indicating that LQ solution is a subset of OCS control allocation structure marked in (19).

Remark 7. The OCS control allocation technique can be regarded as the solution to a more general objective J'_{uy} with incremental cost H_{y} on $\mathbf{y}$ and $\mathbf{y}_{\mathrm{d}}$, i.e.

$$J'_{\mathrm{uy}} = \frac{1}{2}\int_0^{+\infty}\left(H_{\mathrm{y}}(\mathbf{y}, \mathbf{y}_{\mathrm{d}}) + \mathbf{u}^{\mathrm{T}}\mathbf{R}\mathbf{u}\right)dt. \tag{43}$$

Similar to derivations in Theorem 1, the two-stage framework is preserved in its optimal solution structure as

$$\begin{aligned}&\hat{\mathbf{u}} = \mathbf{R}^{-1}\mathbf{G}^*\boldsymbol{\tau};\\ &\boldsymbol{\tau} = -\frac{\partial H_{\mathrm{y}}}{\partial \mathbf{y}}.\end{aligned} \tag{44}$$

This generalization of the linear case in (18)(19) indicates that, in OCS control allocation, the virtual control input τ can be generated in various ways to meet different control performance requirements.

4. Differences between LQ framework and OCS control allocation in practical implementation

While Theorem 2 has shown that $\hat{\mathbf{u}}$ for LQ control (13) is identical to $\hat{\mathbf{u}}$ for OCS control allocation (18)(19), they approach the computation of $\hat{\mathbf{u}}$ from different perspectives. The LQ control technique depends on perfect knowledge/model of internal states $\mathbf{x}$, disturbance $\mathbf{d}$, reference $\mathbf{y}_{\mathrm{d}}$, and the exo-system. This information may not be available in practical implementation. In such a scenario, observers are utilized to estimate (approximate) these states. Assume a typical Kalman filter with observer gain $\mathbf{L}$, the observed state $\mathbf{x}_{\mathrm{o}}$ follows given dynamics

$$\dot{\mathbf{x}}_{\mathrm{o}} = \left(\mathbf{A} - \mathbf{B}_1\mathbf{R}^{-1}\mathbf{B}_1^{\mathrm{T}}\mathbf{P}_1\right)\mathbf{x}_{\mathrm{o}} + \mathbf{L}\left(\mathbf{y} - \mathbf{C}\mathbf{x}_{\mathrm{o}}\right). \tag{45}$$

The observer minimizes the covariance of the state estimation error (Anderson & Moore, 1971), and essentially establishes a relationship from $\mathbf{y}$ to $\mathbf{u}$, given by the transfer function

$$\mathbf{G}_{\text{kf}}(s) \triangleq \mathbf{B}_1^{\text{T}}\mathbf{P}_1\left(s\mathbf{I}-\mathbf{A}+\mathbf{B}_1\mathbf{R}^{-1}\mathbf{B}_1^{\text{T}}\mathbf{P}_1+\mathbf{LC}\right)^{-1}\mathbf{L}\mathbf{Q}_{\text{y}}^{-1}, \tag{46}$$

such that $\mathbf{u}(s) = -\mathbf{R}^{-1}\mathbf{G}_{\text{kf}}\mathbf{Q}_{\text{y}}\mathbf{y}(s)$, which is in the same form as the control allocation structure specified in Theorem 1. Accordingly, $\mathbf{G}_{\text{kf}}$ is an approximation of $\mathbf{G}^*$ from the realization through an optimal state observer guaranteeing closed-loop stability.

Remark 8. Frequency-dependent weights can be added to formula (45) and (46) by augmenting $\mathbf{A}$, $\mathbf{B}_1$, and $\mathbf{C}$ as

$$\widetilde{\mathbf{A}} = \begin{bmatrix}\mathbf{A} & \mathbf{B}_1\mathbf{C}_{\text{w}}\\ \mathbf{0} & \mathbf{A}_{\text{w}}\end{bmatrix},\ \widetilde{\mathbf{B}}_1 = \begin{bmatrix}\mathbf{B}_1\mathbf{D}_{\text{w}}\\ \mathbf{B}_{\text{w}}\end{bmatrix},\ \widetilde{\mathbf{C}} = \begin{bmatrix}\mathbf{C} & \mathbf{0}\end{bmatrix}, \tag{47}$$

where $\mathbf{A}_{\text{w}}$, $\mathbf{B}_{\text{w}}$, $\mathbf{C}_{\text{w}}$, and $\mathbf{D}_{\text{w}}$ formulate a state-space realization of the frequency dependent weight.

On the other hand, the practical implementation of OCS control allocation requires a causal approximation of $\mathbf{G}^*$, which cannot be evaluated going forward in time. The dynamic control allocation method in (Zaccarian, 2009) can be interpreted as an approximation guaranteeing convergence to the DC gain of $\mathbf{G}^*$. Alternatively, OCS control allocation strives to approximate $\mathbf{G}^*$in broadband using, for instance, a causal approximation of $\mathbf{G}^*$ (Duan & Okwudire, 2016a,b) and a proxy-based approximation through feedforward and/or feedback regulation (Duan & Okwudire, 2018). While accurately approximating $\mathbf{G}^*$ is an obvious measure of nearness to total cost optimality, it is shown in (Duan & Okwudire, 2017) that deviation from the optimal subspace defined in (9) is also a useful metric in measuring the energy optimality. Specifically, it is shown that the two-norm squared of the deviation from the optimal subspace is directly proportional to the deviation of J_{u} in (8) from its optimal value.

Unlike LQ methods in which stability is inherently guaranteed, only a subset of approximation of $\mathbf{G}^*$ can guarantee closed-loop stability. This subset is specified through Youla–Kucera parameterization (Doyle, Francis, & Tannenbaum, 2013) in Lemma 2, and stabilizing approximation $\mathbf{G}_{\text{ap}}$ is generated within this subset.

Lemma 2. *[Youla–Kucera Parameterization] For system $\mathbf{G}$, there exist coprime left coprime factors $\mathbf{N}_{\text{L}}(s)$, $\mathbf{D}_{\text{L}}(s)$ and right coprime factors $\mathbf{N}_{\text{R}}(s)$, $\mathbf{D}_{\text{R}}(s)$ (i.e. $\mathbf{G} = \mathbf{D}_{\text{L}}^{-1}\mathbf{N}_{\text{L}} = \mathbf{N}_{\text{R}}\mathbf{D}_{\text{R}}^{-1}$) which formulate the Bézout identity*

$$\begin{bmatrix}\mathbf{X}_{\text{R}} & \mathbf{Y}_{\text{R}}\\ -\mathbf{N}_{\text{L}} & \mathbf{D}_{\text{L}}\end{bmatrix}\begin{bmatrix}\mathbf{D}_{\text{R}} & -\mathbf{Y}_{\text{L}}\\ \mathbf{N}_{\text{R}} & \mathbf{X}_{\text{L}}\end{bmatrix} = \mathbf{I}, \tag{48}$$

where $\mathbf{N}_{\text{L}}$, $\mathbf{D}_{\text{L}}$, $\mathbf{N}_{\text{R}}$, $\mathbf{D}_{\text{R}}$, $\mathbf{X}_{\text{L}}$, $\mathbf{Y}_{\text{L}}$, $\mathbf{X}_{\text{R}}$, $\mathbf{Y}_{\text{R}}$ are all proper and stable linear systems, in which $\mathbf{D}_{\text{L}}$ and $\mathbf{D}_{\text{R}}$ are square and invertible. All stabilizing controllers can be written as

$$\begin{aligned}\mathbf{C}_0 &= \left(\mathbf{Y}_{\text{L}}+\mathbf{D}_{\text{R}}\boldsymbol{\Delta}\right)\left(\mathbf{X}_{\text{L}}-\mathbf{N}_{\text{R}}\boldsymbol{\Delta}\right)^{-1}\\ &= \left(\mathbf{X}_{\text{R}}-\boldsymbol{\Delta}\mathbf{N}_{\text{L}}\right)^{-1}\left(\mathbf{Y}_{\text{R}}+\boldsymbol{\Delta}\mathbf{D}_{\text{L}}\right),\end{aligned} \tag{49}$$

where $\boldsymbol{\Delta}$ is an arbitrary stable and proper system of appropriate size.

Remark 9. The proof and implementation of Youla–Kucera parameterization are detailed in (Doyle et al., 2013). It guarantees closed-loop stability, and indicates a stabilizing approximation of $\mathbf{G}^*$ (i.e. $\mathbf{G}_{\text{ap}}(s)$), given by

$$\mathbf{G}_{\text{ap}}(s) = \mathbf{R}\mathbf{C}_0\mathbf{Q}_{\text{y}}^{-1}. \tag{50}$$

Theorem 3. *Following Youla–Kucera parameterization given by Lemma 2 and $\mathbf{G}_{\text{ap}}$ defined as (50), there always exist $\boldsymbol{\Delta}$ guaranteeing that control $\mathbf{u}$ lies within the optimal control subspace defined in (9), if*

$$n_{\Delta} \geq \left\lceil n_{\text{y}}\left(n_{\text{DR}}+n_{\text{PR}}\right)/n_{\text{r}}\right\rceil - 1, \tag{51}$$

where n_{Δ}, n_{DR}, and n_{PR} are the order of the $\boldsymbol{\Delta}$, $\mathbf{D}_{\text{R}}$, and $\mathbf{G}_{\text{p}}^{-1}\mathbf{G}_{\text{r}}$, respectively, and $\lceil\ \rceil$ indicates the rounding up operation to an integer.

Proof. To construct stable and proper $\mathbf{N}_{\text{L}}$, $\mathbf{D}_{\text{L}}$, $\mathbf{N}_{\text{R}}$, $\mathbf{D}_{\text{R}}$, $\mathbf{X}_{\text{L}}$, $\mathbf{Y}_{\text{L}}$, $\mathbf{X}_{\text{R}}$, $\mathbf{Y}_{\text{R}}$, it is common to first convert system $\mathbf{G}(s)$ to $\mathbf{G}(\lambda)$ using transformation

$$\lambda = \frac{1}{s+1} \Rightarrow s = \frac{1-\lambda}{\lambda}. \tag{52}$$

System $\mathbf{G}(\lambda)$ can be decomposed into polynomial matrix fraction description (Kailath, 1980) $\mathbf{N}_{\text{L}}(\lambda)$, $\mathbf{D}_{\text{L}}(\lambda)$, $\mathbf{N}_{\text{R}}(\lambda)$, $\mathbf{D}_{\text{R}}(\lambda)$, which yields stable and proper $\mathbf{N}_{\text{L}}(s)$, $\mathbf{D}_{\text{L}}(s)$, $\mathbf{N}_{\text{R}}(s)$, $\mathbf{D}_{\text{R}}(s)$ given reverse transformation given by (52). In this condition, the polynomial order of $\mathbf{D}_{\text{R}}(\lambda)$ equals the system order n_{DR}. Define $\boldsymbol{\Delta}$ to be polynomials of λ with order n_{Δ}, in which there are $(n_{\Delta}+1)n_{\text{y}}n_{\text{u}}$ independent variables. The conditions of optimal control subspace (9) can be summarized to be a set of linear constraints on these variables, and its maximum quantity equals $(n_{\text{DR}}+n_{\text{PR}}+n_{\Delta}+1)n_{\text{y}}^2$. This set of linear equations will have a solution if

$$\left(n_{\text{DR}}+n_{\text{PR}}+n_{\Delta}+1\right)n_{\text{y}}^2 \leq \left(n_{\Delta}+1\right)n_{\text{u}}n_{\text{y}}, \tag{53}$$

which is equivalent to (51) based on (6). ■

Remark 10. When n_{Δ} is strictly larger than the condition specified in (51), more degrees of freedom can be used to minimize the approximation error of $\mathbf{G}_{\text{ap}}$ at selected frequencies. It is common to enforce this constraints on DC component (i.e. $\mathbf{G}_{\text{ap}}(0) = \mathbf{G}^*(0)$) to ensure static optimal control allocation.

Example 1. Consider a dual-input, single-output (DISO) system derived from a truncation of the 3-input system in Zaccarian (2009). The state-space representation is

$$\left[\begin{array}{c|c}\mathbf{A} & \mathbf{B}_{\text{l}}\\ \hline \mathbf{C} & \mathbf{D}\end{array}\right] = \left[\begin{array}{cc|cc}-0.157 & -0.094 & 0.87 & 0.253\\ -0.416 & -0.45 & 0.39 & 0.354\\ \hline 0 & 1 & 0 & 0\end{array}\right]. \tag{54}$$

The weighting matrices in Problem 1 are assumed to be $\mathbf{R} = \text{diag}[1, 2]$ and $\mathbf{Q}_{\text{y}} = 10^3$. Assume a disturbance is applied to the first channel of the control input (i.e. $\mathbf{G}_{\text{d}} = G_1$) as

$$d = S + w_0, \tag{55}$$

where S indicates a Heaviside function introducing a step at time $t = 1$ s, while w_0 is assumed to be a low pass filtered white noise signal with 10 Hz bandwidth. This combination introduces a broadband disturbance which is used to compare the performance of different allocation schemes. The filtered white noise w_0 is realized by adding a first-order Butterworth low pass filter to a white noise signal with variance $\sigma^2 = 100$. The following allocator designs are compared:

(i) Kalman filter design $\mathbf{G}_{\text{kf}}$: The formulas in (46) and (47) are adopted with weights comprising an integrator combined with the first-order Butterworth low pass filter (discussed above) according to Remark 8. Disturbance and output covariance matrices are set to be $\mathbf{Q}_{\text{n}} = 10^3$ and $\mathbf{R}_{\text{n}} = 1$, respectively.

(ii) OCS design $\mathbf{G}_{\text{ap}}$: $\mathbf{G}_{\text{ap}}$ is designed to guarantee closed-loop stability through Youla–Kucera parameterization. It minimizes the distance to the OCS defined in (9) while approximating $\mathbf{G}^*$ as much as possible over 0–10 Hz.

To design a stabilizing $\mathbf{G}_{\text{ap}}$, following the transformation defined in (52) and polynomial matrix fraction description, $\mathbf{D}_{\text{R}}$, $\mathbf{Y}_{\text{L}}$, $\mathbf{N}_{\text{R}}$, and $\mathbf{X}_{\text{L}}$ are calculated as

$$\begin{aligned}&\mathbf{D}_{\text{R}} = \begin{bmatrix}\lambda+0.1742 & 0.6144\\ -4.073 & \lambda-2.945\end{bmatrix},\ \mathbf{Y}_{\text{L}} = \begin{bmatrix}-2.2191\\ 4.4232\end{bmatrix},\\ &\mathbf{N}_{\text{R}} = \begin{bmatrix}-1.3738\lambda & -0.8029\lambda\end{bmatrix},\ \mathbf{X}_{\text{L}} = 0.5028.\end{aligned} \tag{56}$$

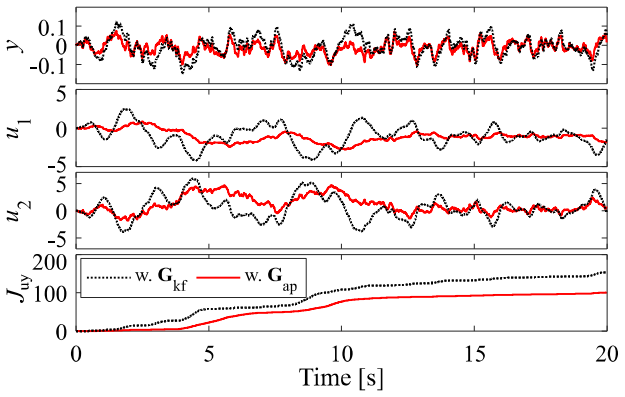

Fig. 2. Comparison of output y, control inputs $\mathbf{u}$ and total cost J_{uy} for Kalman filter approximations $\mathbf{G}_{kf}$ and OCS design $\mathbf{G}_{ap}$.

Accordingly, stabilizing controller $\mathbf{C}_0$ is constructed by Youla–Kucera parameterization as given by (49). According to Theorem 3, n_Δ should be selected to be larger than 1 since $n_{DR} = n_{PR} = n_r = n_y = 1$ for this system and parameterization. In the practical implementation, $n_\Delta = 5$ is selected to enhance the approximation of $\mathbf{G}^*$, i.e.

$$\boldsymbol{\Delta}(\lambda) = \begin{bmatrix} \delta_1\lambda^5 + \delta_2\lambda^4 + \delta_3\lambda^3 + \delta_4\lambda^2 + \delta_5\lambda + \delta_6 \\ \delta_7\lambda^5 + \delta_8\lambda^4 + \delta_9\lambda^3 + \delta_{10}\lambda^2 + \delta_{11}\lambda + \delta_{12} \end{bmatrix}, \tag{57}$$

where $\boldsymbol{\delta} = \{\delta_i\}$ $(i = 1, 2, \ldots, 12)$ are the coefficients to be determined, and they formulate 8 linear equations satisfying the optimal control subspace defined in (9), written as $\mathbf{A}_{OCS}\boldsymbol{\delta} = \mathbf{b}_{OCS}$. To encourage $\mathbf{G}_{ap}(j\omega)$ to approach $\mathbf{G}^*(j\omega)$ from 0–10 Hz,

$$\mathbf{R}(\mathbf{Y}_L + \mathbf{D}_R\boldsymbol{\Delta}) \sim \mathbf{G}^*\mathbf{Q}_y(\mathbf{X}_L - \mathbf{N}_R\boldsymbol{\Delta}) \tag{58}$$

is prescribed according to definition (49) and (50). Note that (58) is also linear with respect to δ, hence can be written as $\mathbf{A}_{ap}(\omega)\boldsymbol{\delta} \sim \mathbf{b}_{ap}(\omega)$ for a given frequency. Accordingly, $\mathbf{G}_{ap}$ is solved as a constrained least square problem, i.e.

$$\min \left\| \begin{bmatrix} \mathbf{A}_{OCS} \\ \mathbf{A}_{ap}(\omega_1) \\ \vdots \\ \mathbf{A}_{ap}(\omega_N) \end{bmatrix} \boldsymbol{\delta} - \begin{bmatrix} \mathbf{b}_{OCS} \\ \mathbf{b}_{ap}(\omega_1) \\ \vdots \\ \mathbf{b}_{ap}(\omega_N) \end{bmatrix} \right\| \tag{59}$$

$$\text{s.t. } \mathbf{A}_{ap}(0)\boldsymbol{\delta} - \mathbf{b}_{ap}(0)$$

where $\omega_1 \ldots \omega_N$ are sampled from 0.1 to 10 Hz (in log scale increment of $10^{0.1}$ Hz), $\mathbf{G}_{ap}(0) = \mathbf{G}^*(0)$ is set to be linear constraints as discussed in Remark 10.

System output y, control input $\mathbf{u}$, and total cost J_{uy} for the two designs are shown in Fig. 2 and summarized in Table 1. Note that the OCS design introduces 33% lower regulation error, as well as 24% and 14% lower control efforts on u_1 and u_2, in comparison with the Kalman filter design with frequency dependent weights. To illustrate the rationale behind this improvement, the output y can be decomposed to three components: y_d, y_{u1} and y_{u2}, corresponding to contributions from the disturbance input and control inputs u_1 and u_2, respectively. Fig. 3 shows the alignment of the components of y for $\mathbf{G}^*$, $\mathbf{G}_{kf}$ and $\mathbf{G}_{ap}$ at a representative frequency (1 Hz). Notice that with $\mathbf{G}^*$ two conditions are satisfied simultaneously: (i) y_{u1} and y_{u2} are aligned in the opposite direction of y_d, and (ii) $|y_{u1}/y_{u2}|$ equals the ratio of control cost according to the OCS defined in (9); these two conditions lead to optimal regulation and control energy. Since such perfect alignment is not possible at every frequency, through the optimization in (59), $\mathbf{G}_{ap}$ seeks to approximate these two conditions as best possible. In comparison, the components of the $\mathbf{G}_{kf}$ are far off target, leading to larger control energy and worse regulation. As a result, the OCS design reduces the total cost by 34% in comparison with the Kalman filter design.

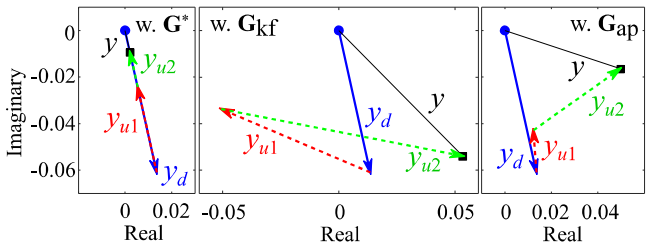

Fig. 3. Control alignment illustration with $\mathbf{G}^*$, $\mathbf{G}_{kf}$ and $\mathbf{G}_{ap}$ at 1 Hz.

Table 1
System output y, control inputs $\mathbf{u}$ and total cost J_{uy} for Kalman filter approximations $\mathbf{G}_{kf}$ and OCS design $\mathbf{G}_{ap}$.

	y (rms)	u_1 (rms)	u_2 (rms)	J_{uy}
w. $\mathbf{G}_{kf}$	0.054	1.72	2.18	154
w. $\mathbf{G}_{ap}$	0.036	1.31	1.88	101

5. Conclusion

The connections between the control allocation and linear quadratic (LQ) control frameworks for optimally distributing control inputs in weakly input redundant systems are explored. It is analytically shown that, for a representative class of exogenous disturbance and references, the LQ control technique is identical to the optimal control subspace (OCS) based control allocation technique. However, for this equivalence to hold, the OCS based control allocation requires evaluation of a (generally) non-causal relationship between control inputs, while the LQ control technique requires perfect knowledge of the system, disturbance and reference states. Neither of these conditions is practically tenable, therefore, approximations are needed. In this regard, the OCS based control allocation technique can be stably realized through Youla–Kucera parameterization while guaranteeing optimal control subspace among the redundant actuators, given a controller of high enough order. On the other hand, the LQ control technique implicitly approximates the optimal relationship via estimation of states, disturbances and/or reference signals. Using a simulation example, it is shown that the OCS design, in comparison with a classical Kalman filter design, enhances the control performance while reducing control energy through via optimized control alignment and approximation of $\mathbf{G}^*$.

References

Anderson, B. D. O., & Moore, J. B. (1971). *Linear optimal control*. Englewood Cliffs, NJ: Prentice-Hall, Inc..

Beard, R. W. (2002). Linear operator equations with applications in control and signal processing. *IEEE Control Systems Magazine*, *22*(2), 69–79.

Bodson, M. (2002). Evaluation of optimization methods for control allocation. *Journal of Guidance, Control and Dynamics*, *25*(4), 703–711.

Brinkerhoff, R., & Devasia, S. (2000). Output tracking for actuator deficient/redundant systems: multiple piezoactuator example. *Journal of Guidance, Control and Dynamics*, *23*(2), 370–373.

Bryson, A., & Ho, Y. (1975). *Applied optimal control: optimization, estimation, and control*. Blaisdell Publishing Company.

Chen, Y., & Wang, J. (2014). Adaptive energy-efficient control allocation for planar motion control of over-actuated electric ground vehicles. *IEEE Transactions on Control Systems Technology*, *22*(4), 1362–1373.

Doyle, J. C., Francis, B. A., & Tannenbaum, A. R. (2013). *Feedback control theory*. Courier Corporation.

Duan, Z., Huang, L., Yao, Y., & Jiang, Z. P. (2012). On the effects of redundant control inputs. *Automatica*, *48*(9), 2168–2174.

Duan, M., & Okwudire, C. E. (2016a). Correction to energy-efficient controller design for a redundantly-actuated hybrid feed drive with application to machining. *IEEE/ASME Transactions on Mechatronics*, *21*(6), 2999–3000.

Duan, M., & Okwudire, C. E. (2016b). Energy-efficient controller design for a redundantly-actuated hybrid feed drive with application to machining. *IEEE/ASME Transactions on Mechatronics*, *21*(4), 1822–1834.

Duan, M., & Okwudire, C. (2017). Proxy-based optimal dynamic control allocation for multi-input, multi-output over-actuated systems. In *Proceedings of the ASME 2017 dynamic systems and control conference* (p. V001T03A005).

Duan, M., & Okwudire, C. E. (2018). Proxy-based optimal control allocation for dual-input over-actuated systems. *IEEE/ASME Transactions on Mechatronics*, *23*(2), 895–905.

Galeani, S., & Pettinari, S. (2014). On dynamic input allocation for fat plants subject to multi-sinusoidal exogenous inputs. In *53rd IEEE conference on decision and control* (pp. 2396–2403).

Galeani, S., Serrani, A., Varano, G., & Zaccarian, L. (2015). On input allocation-based regulation for linear over-actuated systems. *Automatica*, *52*(2015), 346–354.

Halevi, Y., Carpanzano, E., & Montalbano, G. (2014). Minimum energy control of redundant linear manipulators. *Journal of Dynamic Systems, Measurement, and Control*, *136*(5), 051016.

Härkegård, O. (2004). Dynamic control allocation using constrained quadratic programming. *Journal of Guidance, Control and Dynamics*, *27*(6), 1028–1034.

Härkegård, O., & Glad, S. T. (2005). Resolving actuator redundancy—optimal control vs. control allocation. *Automatica*, *41*(1), 137–144.

Johansen, T. A., & Fossen, T. I. (2013). Control allocation—a survey. *Automatica*, *49*(5), 1087–1103.

Kailath, T. (1980). *Linear systems. Vol. 156*. Englewood Cliffs, NJ: Prentice-Hall.

Kirk, D. (2012). *Optimal control theory: an introduction*. Mineola, New York: Dover Publications, Inc..

Kothare, M. V., & Morari, M. (1996). *Multiplier theory for stability analysis of anti-windup control systems*. California Institute of Technology.

Petersen, J. A. M., & Bodson, M. (2006). Constrained quadratic programming techniques for control allocation. *IEEE Transactions on Control Systems Technology*, *14*(1), 91–98.

Petersen, K. B., & Pedersen, M. S. (2008). *The matrix cookbook*. Technical University of Denmark.

Ronde, M. J. C., Schneiders, M. G. E., Kikken, E. J. G. J., van de Molengraft, M. J. G., & Steinbuch, M. (2014). Model-based spatial feedforward for over-actuated motion systems. *Mechatronics*, *24*(4), 307–317.

Schneiders, M. G. E., Molengraft, M. J. G. Van De., & Steinbuch, M. (2004). Benefits of over-actuation in motion systems. In *Proceedings of the 2004 American control conference, Vol. 1* (pp. 505–510).

Servidia, P. A., & Pena, R. S. (2005). Spacecraft thruster control allocation problems. *IEEE Transactions on Automatic Control*, *50*(2), 245–249.

Singh, A. K., & Pal, B. C. (2017). An extended linear quadratic regulator for lti systems with exogenous inputs. *Automatica*, *76*, 10–16.

Tagesson, K., Sundstrom, P., Laine, L., & Dela, N. (2009) Real-time performance of control allocation for actuator coordination in heavy vehicles. In 2009 IEEE Intelligent Vehicles Symposium (pp. 685–690).

Zaccarian, L. (2009). Dynamic allocation for input redundant control systems. *Automatica*, *45*(6), 1431–1438.

Zheng, J., Su, W., & Fu, M. (2010). Dual-stage actuator control design using a doubly coprime factorization approach. *IEEE/ASME Transactions on Mechatronics*, *15*(3), 339–348.

Zhou, J., Canova, M., & Serrani, A. (2016). Predictive inverse model allocation for constrained over-actuated linear systems. *Automatica*, *67*, 267–276.

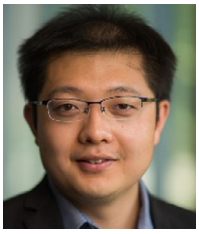

Molong Duan received his B.S. degree from Peking University, Beijing, China, and his M.S.E. and Ph.D. degrees from the University of Michigan (U-M), Ann Arbor, in 2012, 2013 and 2018, respectively. He is currently a research fellow at Aerospace Engineering at U-M. His research interests are control of hybrid and redundantly actuated systems, sustainable manufacturing, intelligent motion command generation, and aeroelasticity. Dr. Duan was granted the Rackham Centennial Fellowship from U-M in 2013. He received the best poster award at the 2014 International Forum on Sustainable Manufacturing and the best student paper award at the 2015 Dynamic Systems and Controls Conference.

Chinedum E. Okwudire received his Ph.D. degree in Mechanical Engineering from the University of British Columbia in 2009 and joined the Mechanical Engineering faculty at the University of Michigan in 2011. Prior to joining Michigan, he was the mechatronic systems optimization team leader at DTL (Mori Seiki, Ltd.) based in Davis, CA. His expertise lies in smart and sustainable automation, where he leverages the fundamental engineering disciplines of machine design, structural dynamics, and control theory to tackle challenging problems in precision, throughput, and energy-efficiency faced by the manufacturing and vehicle automation industries. His scholarly and teaching contributions have been recognized by several awards that include the International Symposium on Flexible Automation Young Investigator Award; the Society of Manufacturing Engineers Outstanding Young Manufacturing Engineer Award; the SAE International Ralph Teetor Educational Award; the National Science Foundation CAREER award; and a number of best paper awards.